


RESEARCH ARTICLE

Supplementary Material: Analyzing Climate Scenarios Using Dynamic Mode Decomposition with Control

Nathan Mankovich¹ , Shahine Bouabid², Peter Nowack³, Deborah Bassotto¹ and Gustau Camps-Valls¹

¹Image Processing Laboratory, Universitat de València, València, Spain

²Department of Earth, Atmospheric, and Planetary Science, Massachusetts Institute of Technology, Cambridge, US

³Institute of Theoretical Informatics & Institute of Meteorology and Climate Research, Karlsruhe Institute of Technology, Karlsruhe, Germany

Received xx xxx xxxx

Keywords: Dynamic mode decomposition, Linear inverse models, Emissions scenario, Temperature, Control

1. Further Experiments with DMDc

We choose $M = 5$ as a reasonable threshold for truncating the singular value decomposition of X' because it sits just after the elbow for the singular value distribution of each scenario (see Fig. 1).

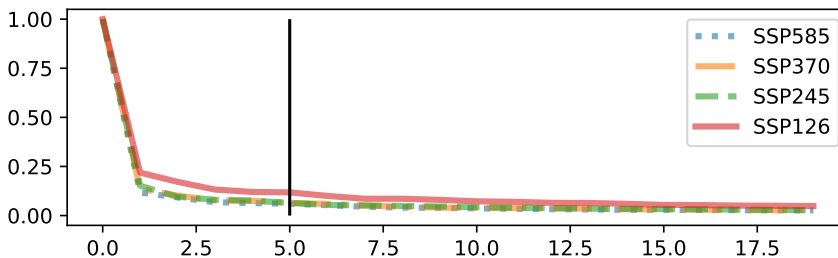
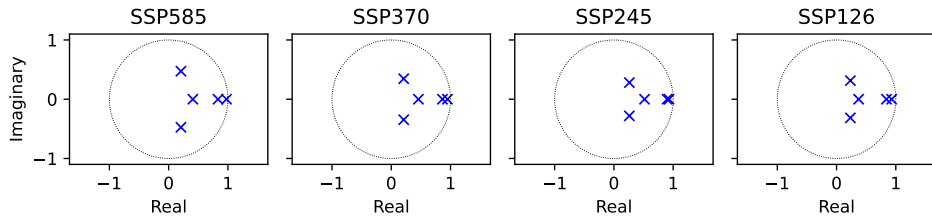


Figure 1. The first 20 normalized singular values of X' . We normalize by dividing by the maximum singular value. The vertical black line represents our singular value threshold of $M = 5$.

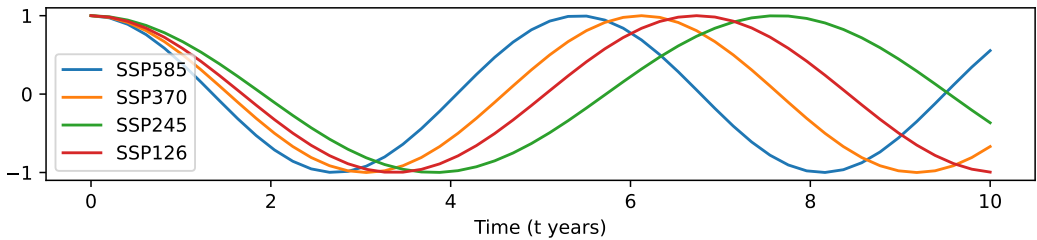
We use a lag of $\tau = 1$ year for the autoregressive component (e.g., to construct X and X') because using more than one year would capture more climatology than we already do. Our aim for this part of the model is to capture internal variability. Internal variability does not have memory, therefore we do not include higher time lags. In experiments, we found that, even with this lag, the autoregressive component captures two phenomena. It captures changes in the warming trend between different scenarios and changes in internal variability in different scenarios (e.g., changes in ENSO oscillation).

01 **1.1. Autoregressive component**

02 The eigenvalues of the DMDc models for each scenario are in Fig. 2. The ENSO modes oscillate at a
 03 higher frequency as we increase the forcing in all scenarios except SSP126 (Fig. 3 and Tab. 1).
 04



05
06
07
08
09
10
11
12
13
14 **Figure 2.** The eigenvalues of the DMDc models.



15
16
17
18
19
20
21
22
23
24
25
26
27
28 **Figure 3.** The oscillation of the ENSO modes over time, based on their eigenvalues from DMDc.

29
30
31 **Table 1.** The frequency of ENSO oscillation for different scenarios detected by DMDc.

| Scenario | Frequency (1/years) |
|----------|---------------------|
| SSP585 | 0.18 |
| SSP370 | 0.16 |
| SSP245 | 0.13 |
| SSP126 | 0.15 |

The least significant scaled mode detected by DMDC is associated with the smallest eigenvalue. We plot this scaled mode in Figure 4 for completeness.

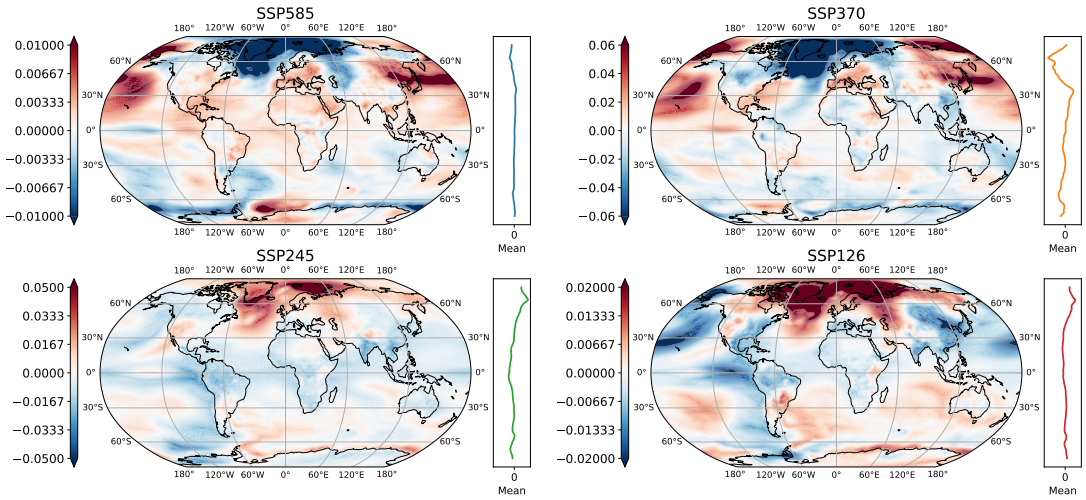


Figure 4. The 5th scaled mode from DMDC. The plot on the right of each map is the mean latitudinal temperature profile. The color bars and latitudinal profiles are in °C.

1.2. Forcing contribution

The DMDC model correctly identifies increased forcing as we increase the emissions scenario. However, it does not identify spatial mean cooling from aerosols (Fig. 5).

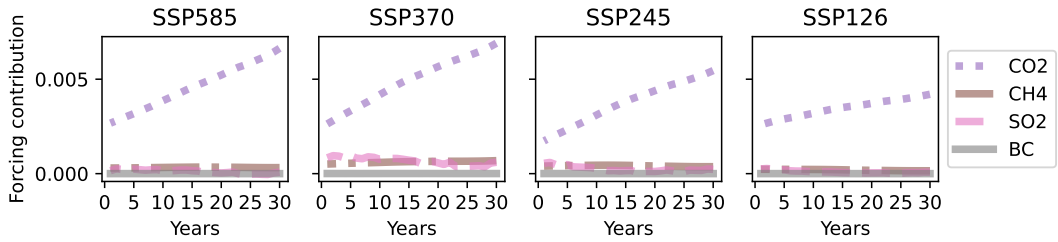


Figure 5. Spatially averaged radiative forcing contribution of each forcing agent for each scenario.

2. Comparison to DMD

We use projected DMD for our DMD model. First, X and X' are constructed as they were for DMDc (see Methods). The DMD model is $x'_n \approx Ax_n$ for $n = 1, 2, \dots, N$. The SVD of X is used to compute the first 5 scaled modes following the procedure by Krake et al. Krake et al. [2021]. The eigenvalues are essentially the same as those from DMDc (Fig. 6).

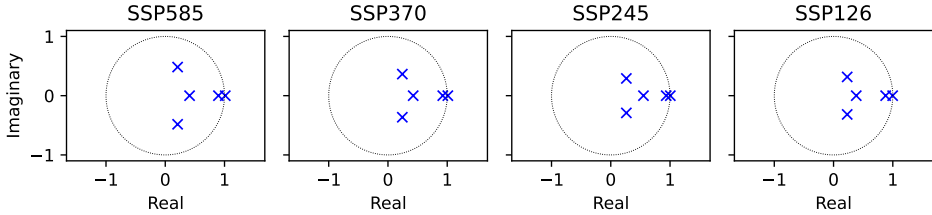


Figure 6. The eigenvalues of the DMD models..

Table 2. The frequency of ENSO oscillation for different scenarios found by DMD.

| Scenario | Frequency (1/years) |
|----------|---------------------|
| SSP585 | 0.19 |
| SSP370 | 0.16 |
| SSP245 | 0.13 |
| SSP126 | 0.15 |

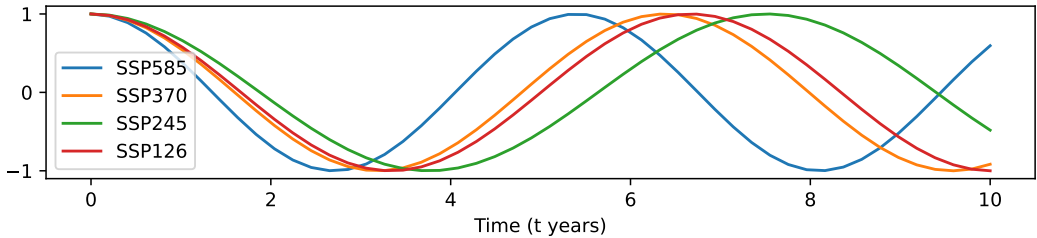
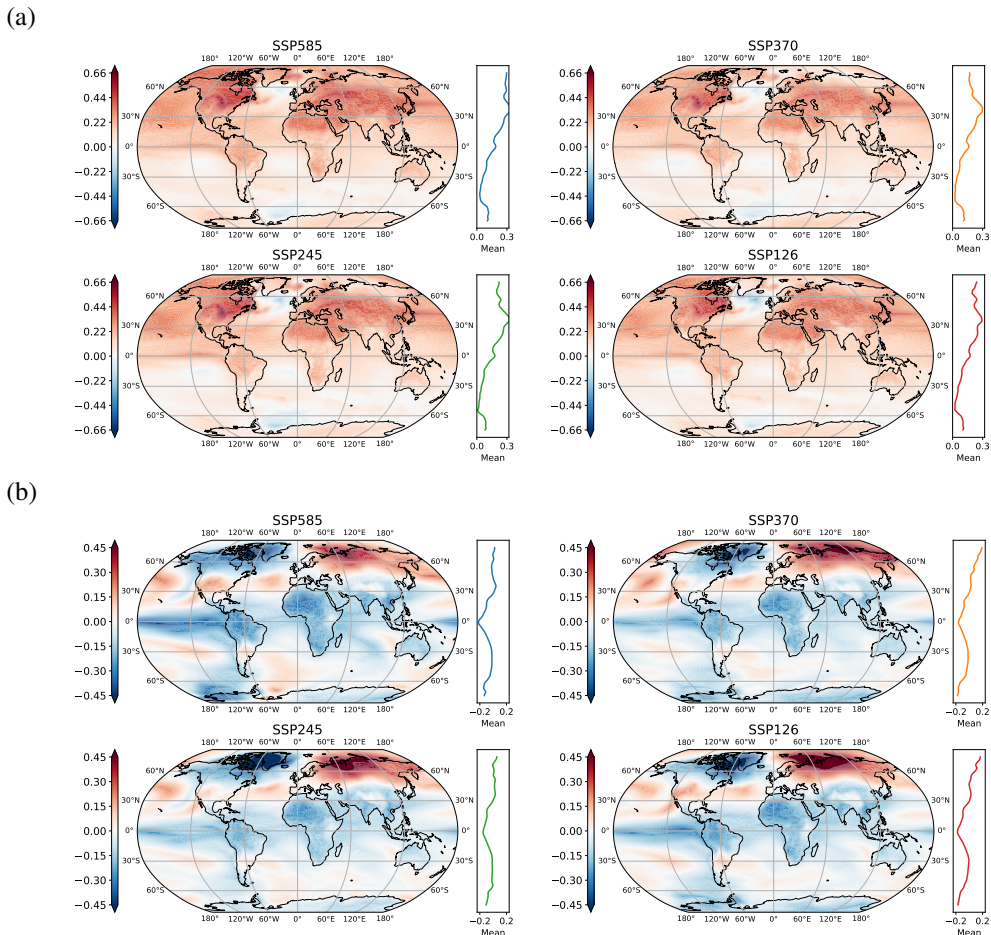


Figure 7. The oscillation of the ENSO modes over time, based on their eigenvalues found by DMD.

01 The warming trend from DMD comes from the sum of warming and cooling scaled modes. This
 02 trend has the same patterns as those found by DMDc and the warming modes have similar correspond-
 03 ing eigenvalues (Fig. 8 a). The two ENSO scaled modes (Fig. 8 b) from DMD display La Niña patterns
 04 and evolve into El Niño after 1 year. These modes oscillate at the same frequency as those from DMDc
 05 except SSP585 (see Tab. 2 and Fig. 7). The major difference between DMD and DMDc lies in the
 06 northern hemisphere of the ENSO patterns. A thorough explanation of this difference is left to future
 07 work. In summary, the scaled modes of DMD exhibit similar spatial patterns and oscillations as those
 08 from DMDc.



41 **Figure 8. Analysis of the scaled modes from DMD.** The scenarios ordered from high to low emissions
 42 are SSP585, SSP370, SSP245, and SSP126. The plot on the right of each map is the mean latitudinal
 43 temperature profile. The color bars and latitudinal profiles are in °C. (a) The warming trend detected by
 44 two scaled modes from DMD. Each spatial pattern is the sum of the two scaled modes associated with
 45 real eigenvalues. (b) ENSO spatial patterns appear in all emissions scenarios, specifically, a La Niña
 46 pattern. Each spatial pattern is the sum of two scaled modes with complex conjugate eigenvalues. All
 47 ENSO patterns evolve into El Niño after 1 year. That is to say, when these scaled modes are scaled by
 48 their associated eigenvalues and added together, we see a clear warming pattern in the central Pacific.
 49

3. DMDc Theory

Proposition 1. *The dynamic modes, φ_m , are the eigenvectors of $\bar{A}\hat{U}\hat{U}^*$ with eigenvalues λ_m .*

Proof.

$$\bar{A}\hat{U}^* \varphi_m = \left(X'V\Sigma^{-1}U_A^* \right) \hat{U}\hat{U}^* \varphi_m \quad (1)$$

$$= \left(X'V\Sigma^{-1}U_A^* \right) \hat{U}\hat{U}^* \left(X'V\Sigma^{-1}U_A^* \hat{U}w_m \right) \quad (2)$$

$$= X'V\Sigma^{-1}U_A^* \hat{U} \underbrace{\hat{U}^* X'V\Sigma^{-1}U_A^* \hat{U}}_{\bar{A}} w_m \quad (3)$$

$$= X'V\Sigma^{-1}U_A^* \hat{U} \underbrace{\tilde{A}w_m}_{\lambda_m w_m} = X'V\Sigma^{-1}U_A^* \underbrace{\hat{U}w_m}_{\varphi_m} \lambda_m = \lambda_m \varphi_m. \quad (4)$$

□

Proposition 2. *$\lambda_m \xi_m$ is the evolution of a scaled mode, ξ_m , over τ time steps in the subspace spanned by the columns of \hat{U} .*

Proof. The DMDc model is $x(t+\tau) = x'_n = Ax_n + By_n = Ax(t) + By_n$ where $t = n + J + \tau - 1$. So an estimation of A using X , Y , and X' , evolves the autoregressive component τ time steps.

We use the projection matrix onto the columns of \hat{U} and the previous proposition to find the evolution of ξ_m in the subspace spanned by the columns of \hat{U} .

$$\bar{A}\hat{U}\hat{U}^* \xi_m = \bar{A}\hat{U}\hat{U}^* \varphi_m \alpha_m = \lambda_m \varphi_m \alpha_m = \lambda_m \xi_m. \quad (5)$$

□

We now provide the reasoning for the decomposition

$$Ax_n \approx \Xi \Lambda \Xi^\dagger x_n. \quad (6)$$

We approximate A with $\bar{A}\hat{U}\hat{U}^*$. From the previous proposition, we have that ξ_m is an eigenvector of $\bar{A}\hat{U}\hat{U}^*$ with eigenvalue λ . By stacking ξ_m into the columns of Ξ and using the pseudoinverse Ξ^\dagger , we have $\bar{A}\hat{U}\hat{U}^* \approx \Xi \Lambda \Xi^\dagger$.

References

Tim Krake, Stefan Reinhardt, Marcel Hlawatsch, Bernd Eberhardt, and Daniel Weiskopf. Visualization and selection of dynamic mode decomposition components for unsteady flow. *Visual Informatics*, 5(3):15–27, 2021.